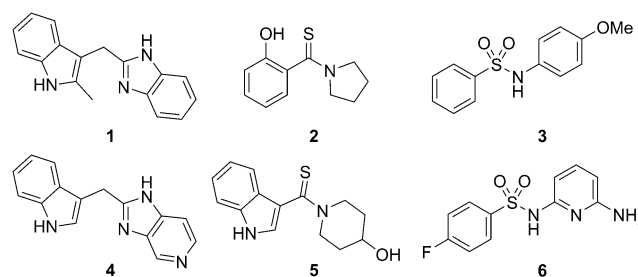


# Discovery of Small Molecules that Bind to K-Ras and Inhibit Sos-Mediated Activation\*\*

Qi Sun, Jason P. Burke, Jason Phan, Michael C. Burns, Edward T. Olejniczak, Alex G. Waterson, Taekyu Lee, Olivia W. Rossanese, and Stephen W. Fesik\*

K-Ras is a small GTPase that functions as a molecular switch cycling between inactive (guanosine diphosphate [GDP]-bound) and active (guanosine triphosphate [GTP]-bound) states. The conversion of K-Ras-GDP to K-Ras-GTP is the rate-limiting step in the activation of K-Ras and is catalyzed by guanine nucleotide exchange factors, such as the son of sevenless (Sos). Mutations in K-Ras fix the protein in the active state and endow cells with capabilities that represent the hallmarks of cancer.<sup>[1]</sup> These include the ability to proliferate, evade apoptosis, reprogram cell metabolism, induce angiogenesis, activate invasion and metastasis, and escape immune destruction.<sup>[2]</sup> Indeed, aberrant K-Ras signaling plays a role in 30% of all human cancers, with the highest incidence of activating mutations found in pancreatic (70–90%), colon (30–50%), and lung (20–30%) carcinomas.<sup>[3]</sup> Downregulation of activated Ras reverses the transformed phenotype of cells and results in the dramatic regression of tumors in murine xenograft models.<sup>[4]</sup> Thus, K-Ras inhibition represents an attractive therapeutic strategy for many cancers. However, Ras activation and signaling is accomplished primarily through protein–protein interactions. Such protein interfaces typically lack well-defined binding pockets and have been difficult to target with small molecules.<sup>[5]</sup>

Herein we report on the discovery of novel small molecules that bind directly to K-Ras between switch I and switch II and inhibit Sos-catalyzed K-Ras activation. To identify compounds that bind directly to K-Ras, we conducted a fragment screen<sup>[6]</sup> using uniformly <sup>15</sup>N-labeled GDP-bound K-Ras (G12D). An NMR-spectroscopy-based screen of 11000 fragments yielded approximately 140 fragments that bind to GDP-bound K-Ras (G12D) (hit rate = 1.3%) as determined by changes of <sup>1</sup>H and <sup>15</sup>N chemical shifts in <sup>1</sup>H/<sup>15</sup>N HSQC spectra of uniformly <sup>15</sup>N-labeled K-Ras (G12D). Representative examples of some of the hits that were identified in the fragment-based screen (**1**, **2**, **3**) as well as analogues that were synthesized to increase water solubility and binding affinity (**4**, **5**, **6**) are depicted in Scheme 1. These compounds bind to K-Ras (G12D) with affinities of 1.3–2 mM.



**Scheme 1.** Multiple chemotypes were identified in the fragment-based screen, including indoles (**1**), phenols (**2**), and sulfonamides (**3**). Analogues of these compounds (**4**, **5**, **6**) were synthesized to increase their water solubility and binding affinity.

The fragment hits identified in the screen were found not only to bind the G12D mutant of K-Ras but also bind to wild-type K-Ras, K-Ras (G12V), and H-Ras (data not shown), thus indicating that these compounds bind to a site that is conserved among Ras isoforms and different K-Ras mutants.

To determine how the fragment hits and analogues bind to K-Ras, we obtained their cocrystal structures. Initial attempts to cocrystallize K-Ras (G12D) with these compounds failed to produce suitable crystals. Owing to the limited number of space groups available to this mutant form of the protein, we performed crystallization screens of both wild-type and G12V mutant K-Ras. Both proteins crystallized across a broad range of conditions in multiple space groups and yielded high-resolution cocrystal structures. In all 20 cocrystal structures obtained thus far, the compounds occupy a hydrophobic pocket located between the  $\alpha$ 2 helix of switch II (60–74) and the central  $\beta$  sheet of the protein. Figure 1a depicts a high-

[\*] Q. Sun,<sup>[a]</sup> Dr. J. P. Burke,<sup>[a]</sup> Prof. J. Phan, M. C. Burns, Prof. E. T. Olejniczak, Prof. T. Lee, Prof. O. W. Rossanese, Prof. S. W. Fesik  
Department of Biochemistry  
Vanderbilt University School of Medicine  
2215 Garland Ave., 607 Light Hall, Nashville, TN 37232 (USA)  
E-mail: stephen.fesik@vanderbilt.edu

Prof. A. G. Waterson  
Department of Pharmacology  
Vanderbilt University School of Medicine  
2200 Pierce Ave., 442 RRB, Nashville, TN 37232 (USA)

[†] These authors contributed equally to this work.

[\*\*] This work was supported by the US National Institutes of Health: SDP1OD006933 (NIH Director's Pioneer Award) to S.W.F., an ARRA stimulus grant (5RC2A148375) to L. J. Marnett, and a NCI SPORE grant in GI cancer (5P50A095103-09) to R.J. Coffey. This work was also funded by the Lustgarten Foundation grant awarded to S.W.F. and the American Cancer Society (Postdoctoral Fellowship, PF1110501CDD) to J.P.B. We thank Matt Mulder (Craig Lindsley lab, Vanderbilt University) for providing HRMS data.

Supporting information (including details of the protein purification, the fragment screen, X-ray crystallography, nucleotide exchange, <sup>1</sup>H/<sup>15</sup>N-HSQC spectra of K-Ras with and without ligands and Sos, and the synthesis of compounds) for this article is available on the WWW under <http://dx.doi.org/10.1002/anie.201201358>.

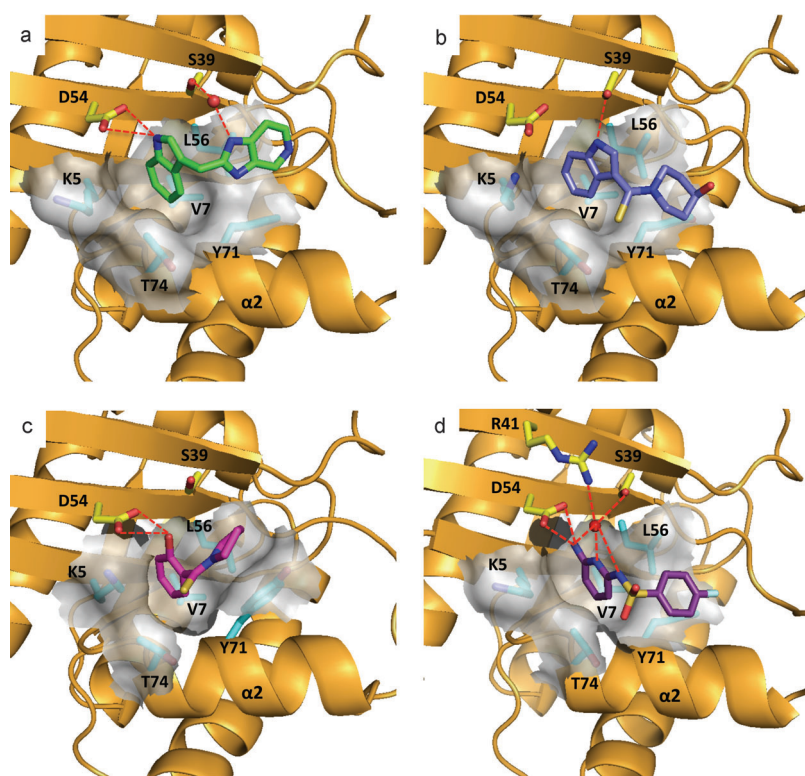


**Figure 1.** Ribbon and molecular surface representations of the X-ray structures of GDP-K-Ras complexed to: a) **4** (PDB code 4EPV), b) **5** (PDB code 4EPW), c) **2** (PDB code 4EPT), and d) **6** (PDB code 4EPX).

resolution structure of **4**, an analogue of the screening hit **1**, complexed to the GDP-bound form of wild-type K-Ras. The indole of **4** binds into a hydrophobic pocket formed by Val-7, Leu-56, and Tyr-71, as well as the aliphatic portion of the side chains of Lys-5 and Thr-74. The imidazopyridine portion of the molecule lies flat in an adjacent binding cleft formed on one side by the side chain of Tyr-71. The nitrogen atom at the 1-position of the imidazopyridine is involved in a water-mediated interaction with the side chain of Ser-39, and the indole NH group forms a hydrogen bond with the side chain of Asp-54. Another member of the indole series (**5**) uses a thiocarbonyl instead of a methylene linker to access the secondary binding cleft. In this case the indole moiety in **5** is rotated towards the  $\alpha 2$  helix and the switch II loop region and forms a hydrogen bond with the side chain of Ser-39 instead of Asp-54. This positions the piperidine ring closer to the helix (Figure 1 b). In addition to an indole, a phenol moiety is also able to bind into this hydrophobic pocket, as demonstrated by the X-ray structure of compound **2** bound to K-Ras (Figure 1 c). The hydroxy group of the phenol forms a hydrogen bond with Asp-54 while the pyrrolidine moiety forms stacking interactions with Tyr-71. The binding mode of a member of the sulfonamide series is shown in Figure 1 d. The pyridine nitrogen atom of **6** forms three water-mediated hydrogen bonds to the side chains of Asp-54, Arg-41, and Ser-39, and the *ortho* amino group interacts with the Asp-54 side chain and a backbone carbonyl group. From these structures, it appears that a hydrogen-bond donor, such as the -NH on the indole moiety or the -OH on the phenol moiety, is important

for binding. This hypothesis is supported by the lack of binding of analogues containing substituents at these positions that occlude hydrogen-bond formation.

Analysis of the ligand-protein cocrystal structures reveal that all the compounds bind to a pocket that is not readily observed in the ligand-free form (Figure 2 a) but in an “open” form of the protein (Figure 2 b). The pocket is created by a conformational change (Figure 2 c) in which the  $\alpha 2$  helix moves away from the central  $\beta$  sheet, and the side chain of Tyr-71 breaks the hydrogen-bond network present in the ligand-free form. Moreover, the side chain of Met-67 rotates out of the way to form a secondary binding cleft. This rotation creates a new binding site for small molecules that is not present in the “closed” form. In subsequent X-ray structures obtained of ligand-free K-Ras under different experimental conditions as well as recently published molecular dynamics simulations, the “open” form has been observed, thus suggesting that the “open” and “closed” conformations are present in equilibrium.<sup>[7]</sup>

The secondary binding cleft is electronegative in character (Figure 2 b) and contains two acidic residues, Glu-37 and Asp-38. To

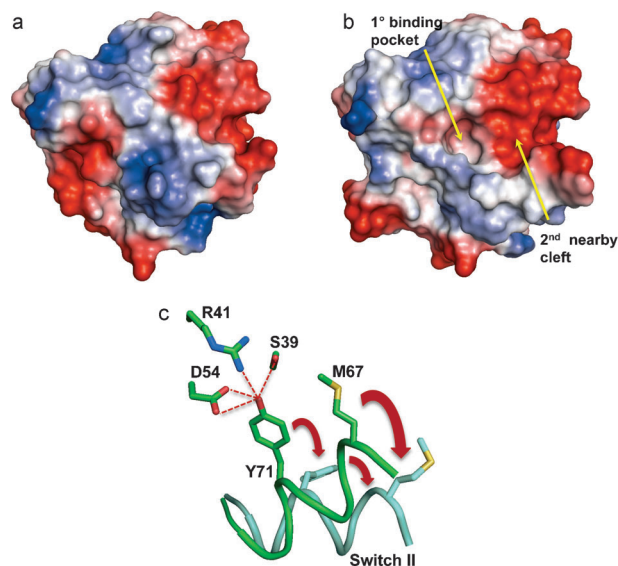
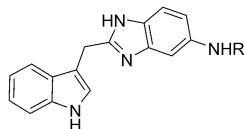


**Figure 2.** Electrostatic surface representations (red negative, blue positive) of GDP-K-Ras a) in the absence of a ligand (PDB code 4EPR) and b) in the “open” form showing the primary hydrophobic binding pocket and the adjacent electronegative cleft. c) Schematic representation of the transition of GDP-K-Ras from the “closed” form (green) to the “open” form (cyan).

bind to this region of the protein, we synthesized amide-linked amino acid analogues of the indole-benzimidazole fragment **7** containing positively charged amine groups (Table 1). Improved binding to K-Ras was observed for

**Table 1:** Compound binding affinity with GDP-K-Ras (G12D) and functional activity in a Sos-catalyzed nucleotide exchange assay.



Compound	R	$K_D$ [ $\mu\text{M}$ ] <sup>[a]</sup>	Inhibition [%] <sup>[b]</sup>
7	-H	$\approx 1300$	no inhibition
8	-Gly	420	$27 \pm 9$
9	-Ala	350	$51 \pm 4$
10	- $\beta$ -Ala	340	$32 \pm 10$
11	-Val	240	$73 \pm 12$
12	-Ile	190	$78 \pm 8$
13	-Pro	340	$58 \pm 8$

[a]  $K_D$  values were measured from the changes in chemical shifts observed in HSQC spectra of uniformly  $^{15}\text{N}$ -labeled protein as a function of added compound. [b] The inhibition in % of Sos-catalyzed nucleotide exchange observed using a 1 mM concentration of compound.

several of these analogues. The best compound in this series contains an isoleucine (**12**) and binds to K-Ras with an affinity of 190  $\mu\text{M}$ , an improvement of roughly 10-fold over the unsubstituted analogue **7**. We were able to obtain a high-resolution X-ray structure of one of these analogues (**13**) complexed to GDP-bound K-Ras (G12V) (Figure 3a). As designed, the indole is located in the primary binding pocket, and the positively charged amino group of the amino acid

interacts with the carboxylic acid side chain of Asp-38 in the secondary binding cleft.

To examine the functional consequences of binding to K-Ras, compounds were tested for their ability to inhibit Sos-mediated nucleotide exchange. In this assay, unlabeled GDP is exchanged for the fluorescently labeled nucleotide BODIPY-GTP; this exchange is catalyzed by Sos and results in an increase in fluorescence.<sup>[8]</sup> As shown in Table 1, the extended analogues with binding affinities below 500  $\mu\text{M}$  inhibited the nucleotide exchange process at a concentration of 1 mM. For example, the analogue containing an isoleucine (**12**) inhibited nucleotide exchange at 78 % (see the Supporting Information). The inhibition of Sos-mediated nucleotide exchange that we observe can be rationalized from a model that was prepared by overlaying the X-ray structure of the K-Ras/**13** complex (Figure 3b) onto a reported structure of H-Ras complexed with Sos.<sup>[9]</sup> The amino acid of **13** clashes with the  $\alpha\text{H}$  helix of Sos. The model predicts that Sos would not be able to bind to K-Ras when complexed to a small molecule that extends into this space (e.g., **8–13**). This model is supported by NMR spectroscopy experiments in which the  $^1\text{H}/^{15}\text{N}$  HSQC spectrum of  $^{15}\text{N}$ -labeled K-Ras (G12D) when complexed to unlabeled Sos dramatically changes upon the addition of compound **13**. This new spectrum resembles that of the K-Ras/**13** complex without Sos (see the Supporting Information). Furthermore, in the absence of K-Ras, compound **13** does not bind to Sos, and an analogue of **13** with the indole moiety N-methylated does not bind to K-Ras and does not inhibit Sos-mediated nucleotide exchange.

In conclusion, by using a fragment-based screen, we have identified small molecules that bind to K-Ras in a hydrophobic pocket that is occupied by Tyr-71 in the apo-Ras crystal structure. Using structure-based design, we obtained analogues of the fragment hits with improved binding affinity as well as functional activity in a Sos-catalyzed nucleotide exchange assay. These compounds bind to K-Ras and block binding to Sos, thereby causing the inhibition of Sos-mediated nucleotide exchange. These molecules represent a starting point for obtaining probe molecules that may be useful in elucidating new insights into Ras signaling and for discovering K-Ras inhibitors for the treatment of cancer.

Received: February 17, 2012

Published online: May 8, 2012

**Keywords:** fragment-based screening · GTPases · K-Ras inhibitors · ligand design · NMR spectroscopy

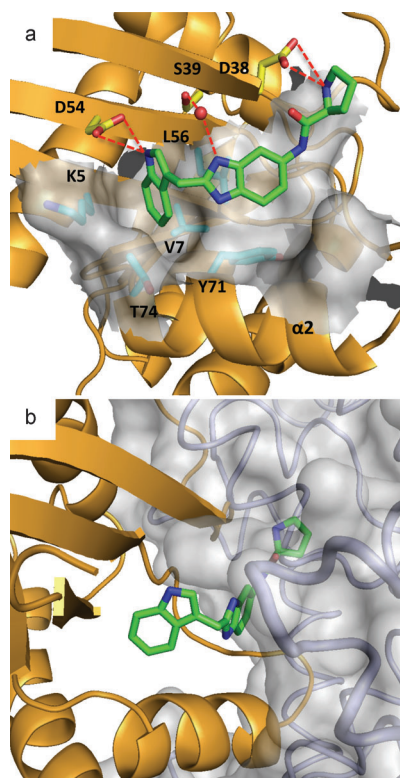


**Figure 3.** a) Ribbon and molecular surface representations of GDP-bound K-Ras complexed to **13** (PDB code 4EPY). b) K-Ras/**13** X-ray structure overlaid with a reported<sup>[9]</sup> H-Ras-Sos complex crystal structure (PDB code 1BKD).

- [1] D. Hanahan, R. A. Weinberg, *Cell* **2011**, 144, 646–674.
- [2] Y. Pylayeva-Gupta, E. Grabocka, D. Bar-Sagi, *Nat. Rev. Cancer* **2011**, 11, 761–774.
- [3] a) L. Laghi, O. Orbetegli, P. Bianchi, A. Zerbi, V. Di Carlo, C. R. Boland, A. Malesci, *Oncogene* **2002**, 21, 4301–4306; b) K. S. Lau, K. M. Haigis, *Mol. Cells* **2009**, 28, 315–320; c) G. J. Riely, J. Marks, W. Pao, *Proc. Am. Thorac. Soc.* **2009**, 6, 201–205; d) J. L. Bos, *Cancer Res.* **1989**, 49, 4682–4689; e) L. C. Yen, Y. H. Uen, D. C. Wu, C. Y. Lu, F. J. Yu, I. C. Wu, S. R. Lin, J. Y. Wang, *Ann. Surg.* **2010**, 251, 254–260.

- [4] a) L. Chin, A. Tam, J. Pomerantz, M. Wong, J. Holash, N. Bardeesy, Q. Shen, R. O'Hagan, J. Pantginis, H. Zhou, J. W. Horner, C. Cordon-Cardo, G. D. Yancopoulos, R. A. DePinho, *Nature* **1999**, *400*, 468–472; b) K. Podsypanina, K. Politi, L. J. Beverly, H. E. Varmus, *Proc. Natl. Acad. Sci. USA* **2008**, *105*, 5242–5247.
- [5] M. R. Arkin, J. A. Wells, *Nat. Rev. Drug Discovery* **2004**, *3*, 301–317.
- [6] a) S. B. Shuker, P. J. Hajduk, R. P. Meadows, S. W. Fesik, *Science* **1996**, *274*, 1531–1534; b) P. J. Hajduk, J. Greer, *Nat. Rev. Drug Discovery* **2007**, *6*, 211–219; c) H. Jhoti, A. Cleasby, M. Verdonk, G. Williams, *Curr. Opin. Chem. Biol.* **2007**, *11*, 485–493.
- [7] a) T. Kigawa, E. Yamaguchi-Nunokawa, K. Kodama, T. Matsuda, T. Yabuki, N. Matsuda, R. Ishitani, O. Nureki, S. Yokoyama, *J. Struct. Funct. Genomics* **2002**, *2*, 29–35; b) J. Ma, M. Karplus, *Proc. Natl. Acad. Sci. USA* **1997**, *94*, 11905–11910.
- [8] A. Patgiri, K. K. Yadav, P. S. Arora, D. Bar-Sagi, *Nat. Chem. Biol.* **2011**, *7*, 585–587.
- [9] P. A. Boriack-Sjodin, S. M. Margarit, D. Bar-Sagi, J. Kuriyan, *Nature* **1998**, *394*, 337–343.
-